PAPER

The effect of ethanol gas impurity on the discharge mode and discharge products of argon plasma jet at atmospheric pressure

IOP Publishing Plasma Sources Science and Technology
Plasma Sources Sci. Technol. **27** (2018) 055001 (7pp) https://doi.org/10.1088/1361-6595/aabdc1

The effect of ethanol gas impurity on the discharge mode and discharge products of argon plasma jet at atmospheric pressure

Wenjie Xia[1], Dingxin Liu[1,4], Han Xu[1], Xiaohua Wang[1], Zhijie Liu[1], Mingzhe Rong[1,4] and Michael G Kong[1,2,3]

[1] State Key Laboratory of Electrical Insulation and Power Equipment, Center for Plasma Biomedicine, Xi'an Jiaotong University, Xi'an 710049, People's Republic of China
[2] Frank Reidy Center for Bioelectrics, Old Dominion University, Norfolk, Virginia 23508, United States of America
[3] Department of Electrical and Computer Engineering, Old Dominion University, Norfolk, Virginia 23529, United States of America

E-mail: liudingxin@mail.xjtu.edu.cn and mzrong@mail.xjtu.edu.cn

Received 15 December 2017, revised 21 March 2018
Accepted for publication 12 April 2018
Published 3 May 2018

Abstract

Argon is a widely used working gas of plasmas, which is much cheaper than helium but on the other hand much more difficult to generate diffuse discharge at atmospheric pressure. In order to meet the application requirements, plenty of researches have been reported to facilitate the diffuse discharge happening for argon plasmas, and in this paper an approach of using ethanol gas (EtOH) impurity is investigated. The discharge characteristics of Ar + EtOH plasma jet are studied as a function of the applied voltage and the concentration of EtOH, from which the concentration of EtOH between ~200 and ~3300 parts per million (ppm) is determined necessary for the generation of diffuse discharge. Compared with the helium plasma jet in literature, it is deduced that the diffuse discharge is probably caused by the Penning ionization happening between the metastable argon and EtOH. The discharge products of Ar + EtOH (672 ppm) plasma jet are measured and the corresponding chemistry pathways are analyzed. About 20% of EtOH is decomposed via complex chemical reactions to form more than a dozen of neutral species, such as CH_3CHO, CH_3COOH, CO, H_2O, and C_nH_{2n+2} ($n \geqslant 3$), and various kinds of ionic species, including C^+, CH^+, ArH^+, O_2^-, $CH_3CH_2O^-$, etc.

Keywords: argon plasma jet, ethanol, diffuse discharge, chemistry pathways

1. Introduction

Atmospheric pressure plasma jets (APPJs) have attracted growing attention in recent years thanks to their promising applications, such as plasma biomedicine [1–5] and material processing [6–10]. Helium is normally used as the working gas of APPJs, because it is easy to generate cold plasmas in the diffuse mode, instead of the filamentary mode which is undesired for most applications. However, helium is too expensive for industry-scale application from an economic standpoint, and hence a cheaper noble gas, argon, is sometimes used as a replacement. The drawback of argon is that it has much higher breakdown voltage than helium, and hence the discharge is easy to transit from diffuse to filamentary [11]. Many researches were reported to control argon plasmas in the diffuse mode. For example, Köhler *et al* [12] and Godyak *et al* [13] reported that the argon diffuse discharge can be realized at low pressure. However, the expensive vacuum system is undesired for applications. Moreover, special plasma sources and electrode structures were developed to overcome this defect, which were operated at atmospheric pressure using pulsed excitation or radio-frequency excitation with a small gas gap of ~1 mm [14–17]. However, these methods still have application limitations that water-cooled electrodes and/or a narrow electrode

[4] Authors to whom any correspondence should be addressed.

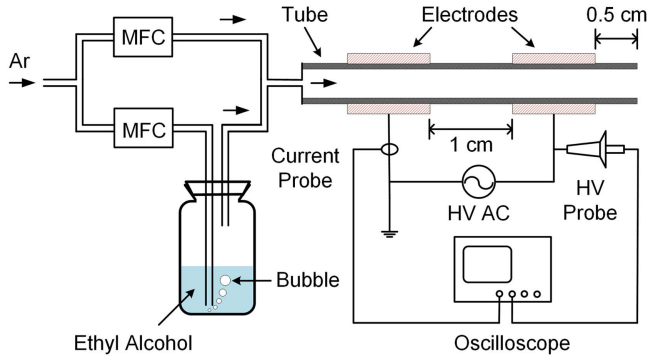

Figure 1. Schematic diagram of the experimental setup.

gap are needed. Interestingly, Glosík *et al* [18] and Sun *et al* [19] showed that the argon diffuse plasmas can be obtained with a lower breakdown voltage by mixing with a small fraction of ethanol (EtOH) at low pressure and atmospheric pressure, respectively. Though the water-cooled electrodes were still used due to the radio-frequency power supply [18, 19], it was found that one way to realize the diffuse discharge of argon APPJ is to add a small amount of gas impurity. Chang *et al* further showed that the Ar plasma jet can be controlled diffuse by adding NH_3 admixture and using an AC power supply without water-cooled electrodes [20]. Therefore, the diffuse discharge of argon can be realized fundamentally in this way, no matter what electrode structures and power supplies are used.

In this paper, a small amount of EtOH gas is mixed in argon for the generation of APPJs, for which the dependence of discharge characteristics on the EtOH concentration and/or the peak-to-peak applied voltage is obtained with emphasis on the discharge mode transition between diffuse and filamentary. Moreover, the discharge products of Ar + EtOH plasmas are measured and their production mechanism is elucidated.

2. Experimental setup

The schematic diagram of the experimental setup is shown in figure 1. The plasma jet device uses a ring–ring electrode structure. Two ring copper electrodes wrap around a quartz tube, which are both 1.0 cm wide and separated from each other by 1.0 cm. The high-voltage electrode is located at downstream side of the gas flow, which is 0.5 cm away from the nozzle of the quartz tube. The quartz tube has 4 mm inner and 6 mm outer diameters, respectively. The working gas consists of premixed argon (5N) and EtOH vapor. Argon flows through two gas tubes into the plasma jet device, each tube contains a mass flow controller (MFC) by which the total gas flow rate is controlled to be 3 l min^{-1}. A bottle of liquid EtOH (purity $\geqslant$ 99.5%) of about 500 ml is connected to one of the gas tube, and hence EtOH vapor can be brought out with the argon gas flow, which is similar to the structure reported by Tsyganov *et al* [21]. It can be estimated that the evaporated EtOH is saturated in argon, because the gas bubbles are very small and they stay for at least 500 ms in the liquid EtOH. Based on the saturation estimation and the gas flow rates through the two gas tubes, the concentration of EtOH after the gas mixing of the two tubes can be evaluated by the Antoine equation and the state equation of ideal gas. The concentration of EtOH can also be varied to a large extent by tuning the two MFCs [22, 23]. The high-voltage electrode is connected to an AC power supply operated at 23 kHz. The peak-to-peak voltage and the discharge current are directly measured by using a high-voltage probe (Tektronix P6015A) and a current probe (Pearson 2877), respectively. In this paper, the average discharge power is mainly kept at 1.0 W, which is obtained by integrating the applied voltage and the discharge current. The discharge images are taken by a digital camera (Nikon D7000), and if the time-resolved images are needed, by an intensified charge-coupled device (Princeton Instruments, PI-Max3). The spectra emitted by the radiative species in the plasma have been detected by an optical emission spectrometer (Andor, SR750) at the nozzle of the quartz tube, and the detected spectral range is between 300 and 800 nm. The effluent gas of the plasma jet is analyzed by a Fourier-transform infrared spectrometer (FTIR, Bruker, Tensor II) in a wave number range of 400–4000 cm^{-1} for both the plasma is on or off. Besides, a molecular beam mass spectrometer (MBMS, Hiden, HPR60) is used to detect the positive and/or negative ions in the plasma plume. For the molecular beam mass spectrum measurements, the quartz tube of the plasma jet device is put vertical to the inlet plate of the MBMS with a separation of 20 mm, and the sampling orifice of the MBMS is located in the axis of the quartz tube.

3. Experimental results

3.1. Comparison of discharge images between the Ar and Ar + EtOH APPJs

Figure 2(a) shows the discharge images of APPJs with the working gases of either Ar or Ar + EtOH. The exposure time of the images is 1.0 s. The concentrations of EtOH are 134, 269, 672 and 3360 parts per million (ppm), respectively. Regarding the Ar or Ar + EtOH (134 ppm) APPJ, the plasma plume does not spew out the nozzle of the quartz tube. Instead, it spews from the ground electrode to the upstream direction of the gas flow. This phenomenon is in accordance with a similar Ar APPJ reported by Shao *et al* [11]. On the contrary, the plasma plume spews out the nozzle of the quartz tube when 269 ppm of EtOH is mixed into Ar, and the plasma plume in open air is lengthened to ~3 cm when the concentration of EtOH further increases to 672 ppm. The phenomenon of plasma spewing out in the high-voltage electrode side is similar to that of the He APPJ, instead of the Ar APPJ, as reported by Shao *et al* [11]. However, when 3360 ppm of EtOH is mixed into Ar, nearly no plasma plume is formed either in the upstream direction or in the downstream direction of the gas flow.

According to the big change of discharge images, it can be hypothesized that the discharge mode is varied with the EtOH concentration from zero to 3360 ppm. This hypothesis

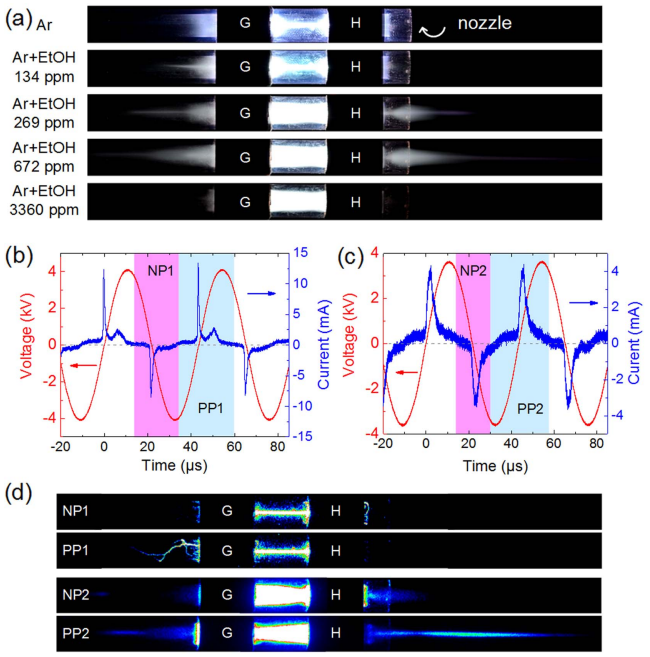

Figure 2. (a) Photographs of APPJs of Ar and Ar + EtOH with an exposure time of 1.0 s. Here, H stands for the high-voltage electrode, and G for the ground electrode. (b), (c) The peak-to-peak voltage and current waveforms of APPJ with the working gas of Ar or Ar + EtOH (672 ppm). (d) The time-resolved images of plasma jets corresponding to the time intervals of NP1, PP1, NP2 and PP2, respectively.

is validated by the time-resolved images for the Ar and Ar + EtOH (672 ppm) plasmas. As shown in figure 2(d), four time-resolved images are taken for the time periods of NP1, PP1, NP2 and PP2, as illustrated in figures 2(b) and (c) in accompany with the applied voltage and current waveforms. At the same discharge power 1.0 W, the peak-to-peak voltage of the Ar and Ar + EtOH (672 ppm) plasmas are 8.3 kV and 7.4 kV, respectively. Each peak in the current waveforms indicates the occurrence of a discharge, so each time period corresponds to the discharge in a half-cycle. It is clear that the Ar plasma is in filamentary mode, while the Ar + EtOH (672 ppm) plasma is in diffuse mode. Therefore, a proper concentration of EtOH admixture could facilitate the generation of diffuse discharge for the Ar-based APPJ.

3.2. The critical parameters of diffuse discharge for the Ar + EtOH APPJ

Figure 3 shows the curves of the breakdown voltage, the threshold voltage for diffuse-to-filamentary transition, and the peak-to-peak voltage at the power of 1.0 W as functions of the EtOH concentration for the Ar + EtOH APPJs. The diffuse discharge can not be fully realized when the EtOH concentration is below 202 ppm, but it can be realized when the peak-to-peak voltage is around 5.9 kV for the EtOH concentration of 202 ppm. With the increase of EtOH concentration, the peak-to-peak voltage range for diffuse discharge is expanded rapidly. When the EtOH concentration is

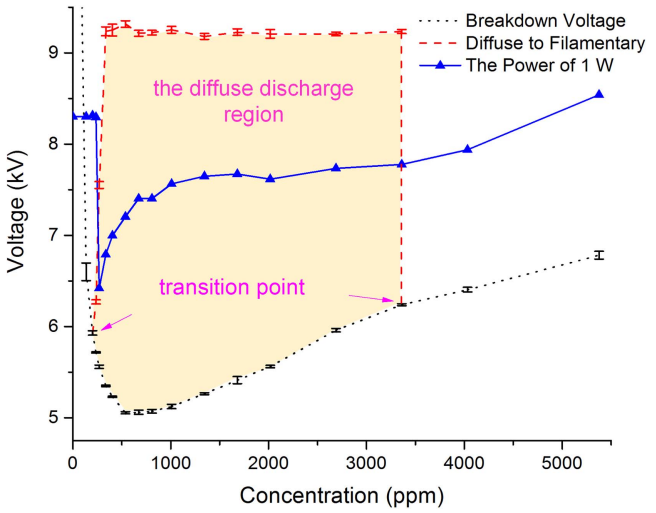

Figure 3. The curves of the breakdown voltage, the threshold voltage for diffuse-to-filamentary transition, and the peak-to-peak voltage at the power of 1.0 W as functions of the EtOH concentration for the Ar + EtOH APPJs. The yellow area indicates the effective ranges of the peak-to-peak voltage and the EtOH concentration for the generation of diffuse discharge.

above 336 ppm, the upper threshold of the peak-to-peak voltage for diffuse discharge is almost stable at 9.2 kV. The lower threshold of the peak-to-peak voltage for diffuse discharge is the breakdown voltage, which decreases with the increase of EtOH concentration. When the EtOH concentration is 672 ppm, the breakdown voltage reaches the minimum value of about 5.0 kV, and then it increases almost linearly to 6.2 kV with the EtOH concentration to 3360 ppm. When the EtOH concentration exceeds 3360 ppm, the diffuse discharge could not be generated, and the growth rate of breakdown voltage slows down. Therefore, it can be concluded that two requirements are roughly needed for the generation of diffuse discharge in Ar + EtOH mixture: (1) the EtOH concentration is between 200 and 3300 ppm and (2) the peak-to-peak voltage is between the breakdown voltage and 9.2 kV.

Besides, the dependence of peak-to-peak voltage on the EtOH concentration at the constant power 1.0 W is also given in figure 3. It can be seen that the discharge transits from filamentary mode into diffuse mode when the EtOH concentration increases to around 260 ppm, and the peak-to-peak voltage decreases sharply to 6.4 kV during the mode transition. This is probably because the diffuse discharge is more uniform than the filamentary discharge, so the conducting channel of the plasma expands. Another reason might be that the diffuse discharge can sustain longer than filamentary discharge as shown in figures 2(b) and (c). The peak-to-peak voltage increases rapidly with the EtOH concentration from 260 to 1000 ppm, and then it is almost constant with the further increase of EtOH concentration from 1000 to 3360 ppm. The discharge mode changes from diffuse to filamentary when the EtOH concentration increases to around 3360 ppm, and then the peak-to-peak voltage turns to rise again due to the shrink of the discharge area.

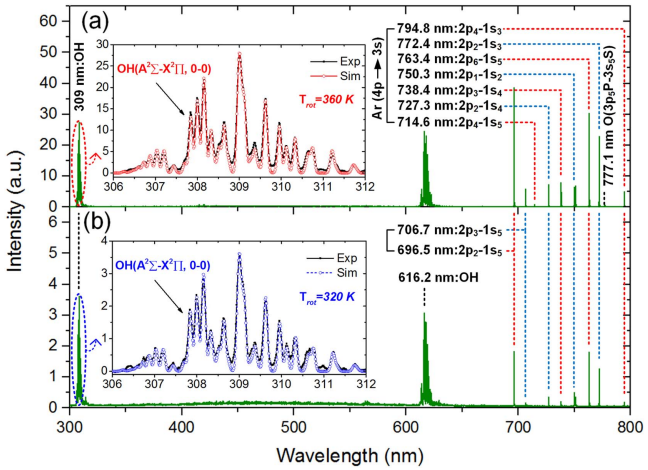

Figure 4. Emission spectra of the (a) Ar and (b) Ar + EtOH (672 ppm) APPJ measured at the nozzle of the quartz tube.

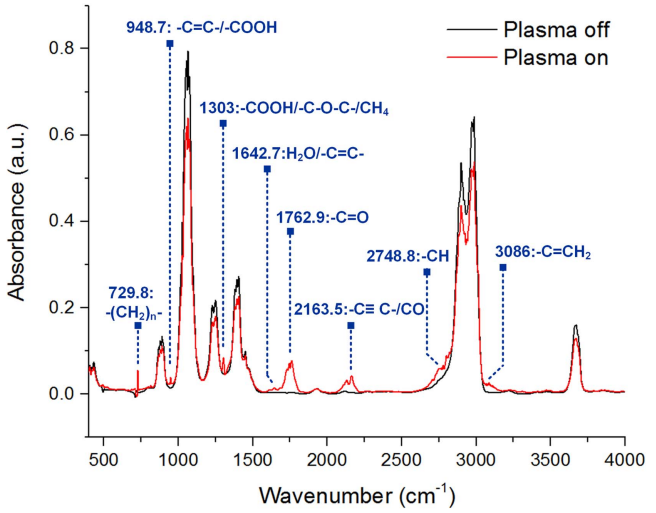

Figure 5. Fourier-transform infrared spectra of Ar + EtOH (672 ppm) effluent gas with or without discharge.

3.3. Analysis of the radiative species in the Ar and Ar + EtOH (672 ppm) APPJs by means of optical emission spectrometry

From an application point of view, it is important to know the composition of discharge products, and hence in this paper they are measured by means of optical emission spectrometry, Fourier-transform infrared spectrometry and molecular beam mass spectrometry. The optical emission spectra of the Ar APPJ at 8.3 kV and the Ar + EtOH (672 ppm) APPJ at 7.4 kV are detected at the nozzle of the quartz tube, and these two plasma jets have the same discharge power of 1.0 W. The spectra are shown in figures 4(a) and (b), respectively. For both cases, the OH band (306–312 nm) and the argon spectral lines are dominant, similar to the result reported by Sun *et al* [19]. It is worth noting that the emission intensity of the Ar APPJ is larger than that of the Ar + EtOH (672 ppm) APPJ by one order of magnitude. Especially, the emission intensity at 695.5 nm (the metastable Ar^*) of the Ar APPJ is 21.5 times of that of the Ar + EtOH (672 ppm) APPJ. Since the emission intensity of a spectral line reflects the relative density of a specific radiative species, the comparison of emission intensities between the Ar and Ar + EtOH (672 ppm) APPJs indicates that the former has much higher densities of OH(A) and Ar^* [17]. This implies that a large amount of Ar^* might be consumed by reacting with EtOH in the Ar + EtOH (672 ppm) APPJ.

Additionally, the gas temperatures of the Ar and Ar + EtOH (672 ppm) APPJs are measured and then compared with each other. For a discharge at atmospheric pressure, the rotational temperature could be assumed as the gas temperature [24]. The OH emission spectra of the Ar and Ar + EtOH (672 ppm) APPJs in the range 306–312 nm have been measured with a high resolution of 0.015 nm, respectively. The measured emission spectra are compared to the theoretical spectra simulated at different gas temperatures using the software namely LIFBASE [25]. The best fits are found to be a temperature of 360 K for the Ar APPJ and a temperature of 320 K for the Ar + EtOH (672 ppm) APPJ. The results indicate that a small amount of EtOH mixed into argon could lower the gas temperature, which benefits the heat-sensitive plasma applications such as plasma biomedicine. It's interesting that the difference in temperature is big but the discharge power is the same for the Ar and Ar + EtOH (672 ppm) APPJs. The possible reason is that larger portion of the electric energy in the Ar + EtOH (672 ppm) APPJ is consumed to decompose the chemical bonds of EtOH, producing new species instead of heating the gas.

3.4. Analysis of the neutral products in the effluent gas of Ar + EtOH (672 ppm) APPJ by means of Fourier-transform infrared absorption spectrometry

For both plasma on and plasma off, the infrared absorption spectra of Ar + EtOH (672 ppm) gas mixture are obtained by injecting the effluent gas into the gas pool of the FTIR. As shown in figure 5, the absorption spectrum of Ar + EtOH (672 ppm) without discharge has spectral bands at around 800–1500, 2700–3000, 3670 cm^{-1}, which are the 'finger prints' of EtOH molecules [26]. When the plasma is turned on, the intensity of these bands drops by around 20%. Since the absorbance is proportional to the gas density according to the Lambert–Beer law, it can be concluded that 20% of EtOH molecules are decomposed in the Ar + EtOH (672 ppm) APPJ. Besides, the absorption bands of some new species are detected when the plasma is on, such as the absorption peak of $-(CH_2)_n-$ ($n \geqslant 3$) at 729.8 cm^{-1}, the absorption peak of –C=C– and/or –COOH at 948.7 cm^{-1}, the absorption peak of H_2O and/or –C=C– at 1642.7 cm^{-1}, and the absorption peaks of –C≡C– and/or CO (gas) at about 2163.5 cm^{-1}. It is worth noting that the absorption peak of –C=O at 1762.9 cm^{-1} and –CH at 2748.8 cm^{-1} are also detected, indicating that acetaldehyde exists in the effluent gas.

3.5. Analysis of the ionic species in the Ar + EtOH (672 ppm) plasma plume by means of molecular beam mass spectrometry

FTIR can only measure long-lived neutral species, which are produced by a series of chemical processes such as ionization,

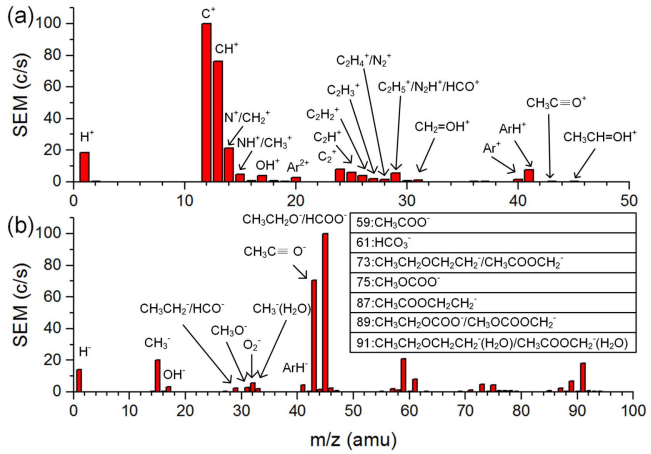

Figure 6. Molecular beam mass spectra of (a) positive ions and (b) negative ions in Ar + EtOH (672 ppm) plasma plume.

decomposition and recombination, it is difficult to deduce the chemical pathways in the plasma based on the neutral products. In order to deepen the understanding of the transient processes in the Ar + EtOH (672 ppm) APPJ, a MBMS is also used to detect the charged products in the plasma plume, and the results are shown in figure 6 [27–29].

Figure 6(a) shows the dominant positive ions with the m/z value from 1 to 50 amu, and the positive ions with the m/z value greater than 50 are not detected. The most abundant peaks correspond to C^+ and CH^+ ($m/z = 12$ or 13). Due to the presence of argon, the peaks corresponding to Ar^+ and Ar^{2+} ($m/z = 40$ or 20) are detected, and the protonated species ArH^+ ($m/z = 41$) is also detected. Besides, the fragment ions of EtOH peak at $m/z = 29$, 31, 43 and 45, corresponding to $HC{\equiv}O^+$, $CH_2{=}OH^+$, $CH_3C{\equiv}O^+$ and $CH_3CH{=}OH^+$, are detected too. Interestingly, Ar_2^+ ($m/z = 80$) is not detected in our experiments, but it is detected by Dünnbier *et al* [29] when using a rf power supply with a discharge power much greater than 1.0 W. The mass spectrum was found to vary significantly with the discharge power, indicating that the production of Ar_2^+ might be sensitive to the discharge power density [30].

Figure 6(b) shows the dominant negative ions with the m/z value from 1 to 100 amu, and the negative ions with the m/z value greater than 100 are almost not detected. The main negative ions are $CH_3CH_2O^-$, $CH_3C{\equiv}O^-$, and CH_3COO^- (with m/z equals to 45, 43 or 59, respectively), which are the deprotonated ions of EtOH, acetaldehyde (CH_3CHO) and acetic acid (CH_3COOH). Besides, the deprotonated ions $C_nH_{2n+1}^-$ ($n \geqslant 3$) are detected, indicating the existence of alkane C_nH_{2n+2} ($n \geqslant 3$). This is in accordance to the measurement result of FTIR (see figure 5), in which the absorption peak of $-(CH_2)_n-$ ($n \geqslant 3$) at 729.8 cm^{-1} are detected. Moreover, hydrated anions such as $CH_3CH_2OCH_2CH_2^-(H_2O)$ and/or $CH_3COOCH_2^-(H_2O)$ ($m/z = 91$) are also detected, which should be produced by the combination of anions and water molecules.

4. Chemistry pathways in Ar + EtOH APPJ

The potential energy of Ar^* ($4^3P_2{}^0$) is 11.56 eV, lower than the ionization energy of N_2 (15.58 eV) and O_2 (12.2 eV). So, Penning ionization is hardly to happen in the Ar APPJ although N_2 and O_2 are inevitably mixed into the working gas, and the main ionization pathway is [18]

$$Ar + e(\text{energy} > 15.8\ \text{eV}) \rightarrow Ar^+ + 2e. \quad (1)$$

However, when a small amount of EtOH is mixed into Ar, Penning ionization is largely possible to happen because the ionization energy of EtOH is just 10.47 eV. Therefore, there should be another two main ionization pathways in Ar + EtOH APPJ, as given by [18, 19, 31]

$$CH_3CH_2OH + e\ (\text{energy} > 10.47\ \text{eV}) \rightarrow PI^+ + NS + 2e, \quad (2)$$

$$CH_3CH_2OH + Ar^* \rightarrow PI^+ + NS + Ar + e, \quad (3)$$

where PI^+ represents the positive ions, NS represents the neutral species, and e represents the electrons. Although the density of EtOH is much lower than Ar, the reaction (2) may have comparable, or even larger rate compared to reaction (1), because the amount of e (energy > 10.47 eV) is higher than that of e (energy > 15.8 eV) by several orders of magnitude. As shown in figure 4, the emission intensity of Ar^* is much higher in the Ar APPJ than that in the Ar + EtOH APPJ. Two chemistry pathways should be responsible for this: (1) a large amount of electrons is consumed by the reactions with EtOH rather than the excitation of Ar, and (2) Ar^* is consumed by EtOH via Penning ionization. These pathways should be very strong since 20% of EtOH is decomposed, as shown in figure 5. Ar^* is neutral and hence not confined in the discharge channel, so the Penning ionization could expand the plasma region, which might be an important factor for the discharge mode transition from filamentary to diffuse.

The negative ion is thought to be produced mainly by electron attachment and proton abstraction, as given by [32]

$$e\ (\text{low} - \text{energy}) + NS \rightarrow NS^-, \quad (4)$$

$$M - H + NS^- \rightarrow M^- + NS - H, \quad (5)$$

where M–H and NS–H represent the H-containing neutral species, and M^- and NS^- represent the negative ions. For example, the dissociative electron attachment of oxygen produces $O_2{}^-$, which can further react with a EtOH molecule to produce a deprotonated ion $CH_3CH_2O^-$ ($m/z = 45$) and a free radical HO_2.

The discharge mechanism of the Ar + EtOH APPJ is complex, and we comment here only briefly on what are likely to be the important chemistry pathways [26, 33, 34]. Based on the experimental findings, the ionization reactions in the Ar + EtOH APPJ could be deduced, as shown in figure 7.

Due to the electron impact ionization and the possible Penning ionization, the chemical bonds of EtOH (CH_3CH_2OH) break to lose a free radical H, OH or CH_3, resulting in the formation of several primary products. These

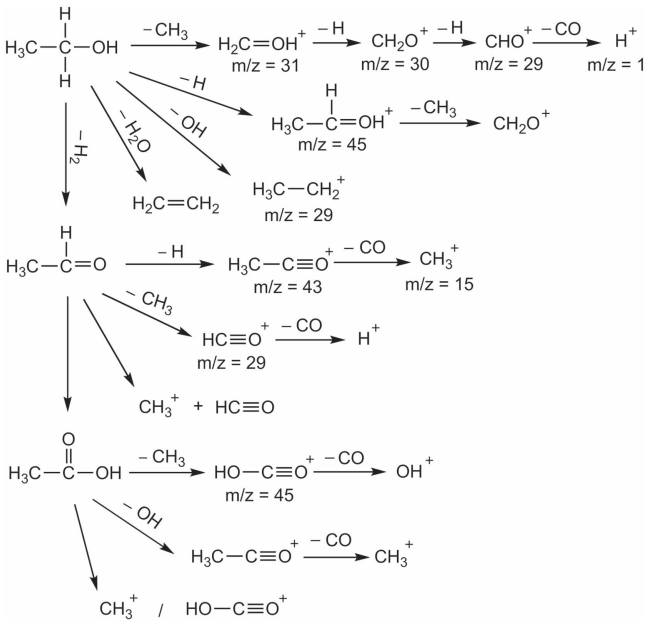

Figure 7. Possible ionization processes in the Ar + EtOH APPJ.

products include the fragment ions, such as $CH_2{=}OH^+$, $CH_3CH{=}OH^+$, and $CH_3CH_2^+$, and the neutral species, such as C_2H_4 and CH_3CHO. Part of the fragment ions are further decomposed into smaller fragment ions, e.g. $CH_2{=}OH^+$ is further decomposed into CH_2O^+ and finally decomposed into H^+ and CO. Also, some neutral species are further decomposed, producing new fragment ions and neutral species. For example, CH_3CHO is further decomposed into fragment ions, such as $CH_3C{\equiv}O^+$, $HC{\equiv}O^+$ and CH_3^+, and neutral species, such as CH_3COOH. The decomposition of CH_3COOH is also similar, which is illustrated in figure 7.

5. Conclusion

A small amount of ethanol gas (EtOH) is mixed into argon to make the argon-based plasma jet transiting from filamentary discharge to diffuse discharge, which is preferable for various plasma applications. The effective concentration of EtOH for diffuse discharge is found to between ~200 and ~3300 ppm, and in that case the plasma plume can spew out from the high-voltage electrode, instead of that from the ground electrode for the Ar APPJ. Compared with the helium APPJ in literature, it is deduced that the diffuse discharge is probably caused by the Penning ionization happening between the metastable Ar^* and the EtOH, which is reasonable because the metastable Ar^* has a potential energy 11.56 eV, higher than the ionization energy of EtOH (10.47 eV). The distribution of metastable Ar^* can not be confined in the discharge channel, and hence benefits to diffuse the plasmas to form diffuse discharge. The effect of Penning ionization is reflected by comparing the optical emission spectrometry and the molecular beam mass spectrometry between Ar and Ar + EtOH (672 ppm) APPJs. With the same discharge power, the emission intensities of metastable Ar^* spectral lines are much lower for the Ar + EtOH (672 ppm) APPJ by at least one order of magnitude, while around 20% of EtOH is decomposed to form various kinds of species including the neutral species, positive ions and negative ions. The positive ions and neutral species, such as C^+, CH^+, CH_2^+, ArH^+, CO, H_2O, CH_3CHO, CH_3COOH and C_nH_{2n+2} ($n \geqslant 3$), are thought to be formed mainly by electron impact ionization and Penning ionization. While the negative ions, such as O_2^-, $CH_3CH_2O^-$, $CH_3C{\equiv}O^-$, CH_3COO^- and $C_nH_{2n+1}^-$, are thought to be formed mainly by dissociative electron attachment, and proton abstraction. Furthermore, the possible chemistry pathways to form these species are given for a better understanding.

This work was supported by the National Natural Science Foundation of China (Grant No. 51521065).

ORCID iDs

Dingxin Liu https://orcid.org/0000-0002-3503-9883
Han Xu https://orcid.org/0000-0002-3525-8904

References

[1] Kong M G, Kroesen G, Morfill G, Nosenko T, Shimizu T, van Dijk J and Zimmermann J L 2009 *New J. Phys.* **11** 115012
[2] Von Woedtke T, Reuter S, Masur K and Weltmann K-D 2013 *Phys. Rep.* **530** 291–320
[3] Lu X, Laroussi M and Puech V 2012 *Plasma Sources Sci. Technol.* **21** 034005
[4] Fridman G, Friedman G, Gutsol A, Shekhter A B, Vasilets V N and Fridman A 2008 *Plasma Process. Polym.* **5** 503–33
[5] He T, Liu D, Liu Z, Liu Z, Liu Z, Li Q R M and Kong M G 2017 *Appl. Phys. Lett.* **111** 203702
[6] Jiang N, Gao L, Ji A and Cao Z 2011 *J. Appl. Phys.* **110** 083301
[7] Walsh J L and Kong M G 2007 *Appl. Phys. Lett.* **91** 251504
[8] Fang Z, Lin J, Xie X, Qiu Y and Kuffel E 2009 *J. Phys. D: Appl. Phys.* **42** 085203
[9] Xu J, Zhang C, Shao T, Fang Z and Yan P 2013 *J. Electrost.* **71** 435–9
[10] Cheng C, Zhang L and Zhan R J 2006 *Surf. Coat. Technol.* **200** 6659–65
[11] Shao X J, Jiang N, Zhang G J and Cao Z X 2012 *Appl. Phys. Lett.* **101** 253509
[12] Köhler K, Coburn J W, Horne D E, Kay E and Keller J H 1985 *J. Appl. Phys.* **57** 59–66
[13] Godyak V A, Piejak R B and Alexandrovich B M 1992 *Phys. Rev. Lett.* **68** 40
[14] Laimer J and Störi H 2006 *Plasma Processes Polym.* **3** 573–86
[15] Laimer J and Störi H 2007 *Plasma Process. Polym.* **4** 266–74
[16] Balcon N, Aanesland A and Boswell R 2007 *Plasma Sources Sci. Technol.* **16** 217
[17] Walsh J L and Kong M G 2007 *Appl. Phys. Lett.* **91** 221502
[18] Glosík J, Pavlík J, Šícha M and Tichý M 1987 *Czech. J. Phys.* **37** 188–93
[19] Sun W T, Li G, Li H P, Bao C Y, Wang H B, Zeng S, Gao X and Luo H Y 2007 *J. Appl. Phys.* **101** 123302
[20] Chang Z, Jiang N, Zhang G and Cao Z 2014 *J. Appl. Phys.* **115** 103301
[21] Tsyganov D, Bundaleska N, Tatarova E and Ferreira C M 2013 *Int. J. Hydrog. Energy* **38** 14512–30
[22] Thomson G W 1946 *Chem. Rev.* **38** 1–39

[23] Zhou Y, Yuan Q, Wang X, Yin G and Dong C 2014 *Plasma Sci. Technol.* **16** 99
[24] Bundaleska N, Tsyganov D, Saavedra R, Tatarova E, Dias F M and Ferreira C M 2013 *Int. J. Hydrog. Energy* **38** 9145–57
[25] Lugue J and Crosley D R 1999 Lifbase: Database and Spectral Simulation Program (ver. 1.6) *Report* MP 99–009 SRI International
[26] Du C M, Mo J M and Li H X 2015 *Chem. Rev.* **115** 1503–42
[27] Jiménez M, Rincón R, Marinas A and Calzada M D 2013 *Int. J. Hydrog. Energy* **38** 8708–19
[28] Jiménez M, Yubero C and Calzada M D 2008 *J. Phys. D: Appl. Phys.* **41** 175201
[29] Dünnbier M, Schmidt-Bleker A, Winter J, Wolfram M, Hippler R, Weltmann K-D and Reuter S 2013 *J. Phys. D: Appl. Phys.* **46** 435203
[30] Malović G, Puač N, Lazović S and Petrović Z 2010 *Plasma Sources Sci. Technol.* **19** 034014
[31] Levko D, Sharma A and Raja L L 2017 *J. Phys. D: Appl. Phys.* **50** 085202
[32] Albert A, Shelley J T and Engelhard C 2014 *Anal. Bioanal. Chem.* **406** 6111–27
[33] Rincón R, Marinas A, Muñoz J, Melero C and Calzada M D 2016 *Chem. Eng. J.* **284** 1117–26
[34] Tatarova1 E, Bundalesk N, Sarrette J P and Ferreira C M 2014 *Plasma Sources Sci. Technol.* **23** 063002